Linking Cognitive Neuroscience and Molecular Genetics: New Perspectives from Williams Syndrome
Ursula Bellugi and Marie St. George (Eds.)

VI. Genome Structure and Cognitive Map of Williams Syndrome

Julie R. Korenberg, Xiao-Ning Chen, and Hamao Hirota
Cedars-Sinai Medical Center and University of California, Los Angeles

Zona Lai and Ursula Bellugi
The Salk Institute for Biological Studies

Dennis Burian and Bruce Roe
University of Oklahoma

Rumiko Matsuoka
Tokyo Women's Medical University

Abstract

■ Williams syndrome (WMS) is a most compelling model of human cognition, of human genome organization, and of evolution. Due to a deletion in chromosome band 7q11.23, subjects have cardiovascular, connective tissue, and neurodevelopmental deficits. Given the striking peaks and valleys in neurocognition including deficits in visual–spatial and global processing, preserved language and face processing, hypersociability, and heightened affect, the goal of this work has been to identify the genes that are responsible, the cause of the deletion, and its origin in primate evolution. To do this, we have generated an integrated physical, genetic, and transcriptional map of the WMS and flanking regions using multicolor metaphase and interphase fluorescence in situ hybridization (FISH) of bacterial artificial chromosomes (BACs) and P1 artificial chromosomes (PACs), BAC end sequencing, PCR gene marker and microsatellite, large-scale sequencing, cDNA library, and database analyses. The results indicate the genomic organization of the WMS region as two nested duplicated regions flanking a largely single-copy region. There are at least two common deletion breakpoints, one in the centromeric and at least two in the telomeric repeated regions. Clones anchoring the unique to the repeated regions are defined along with three new pseudogene families. Primate studies indicate an evolutionary hot spot for chromosomal inversion in the WMS region. A cognitive phenotypic map of WMS is presented, which combines previous data with five further WMS subjects and three atypical WMS subjects with deletions; two larger (deleted for D7S489L) and one smaller, deleted for genes telomeric to *FZD9*, through *LIMK1*, but not *WSCR1* or telomeric. The results establish regions and consequent gene candidates for WMS features including mental retardation, hypersociability, and facial features. The approach provides the basis for defining pathways linking genetic underpinnings with the neuroanatomical, functional, and behavioral consequences that result in human cognition. ■

INTRODUCTION

Williams syndrome (WMS) is one of the most compelling models of human cognition. Given the emerging grasp of the human genome, study of subjects with WMS provides the opportunity to elucidate the pathways that lead from genes to behavior in the cognitive neurosciences. This understanding may ultimately help to shed light on our evolutionary origins and to elucidate a part of what makes us human.

WMS is a particularly powerful model, because it is characterized by specific deficits coupled with remarkably preserved abilities. It provides the opportunity to probe neurocognitive pathways in humans across different levels, including the cellular, physiological, anatomic, functional, and cognitive, with each of these ultimately related to the underlying changes in gene expression. Armed with this information, one can then begin to infer the interconnections and to understand

the molecular basis of human behavior. In this report, the approach to defining the genetic, anatomic, and neurocognitive basis of WMS will be presented along with a physical map and the genomic structure of WMS region. These data will be used to generate a phenotypic map of WMS and to define subsets of genes responsible for a part of the facial features and mental retardation.

Physical Features and Neurocognition in WMS

WMS is a rare genetic disorder that occurs in about one in 20,000 births and is characterized by mental retardation, a hoarse voice, transient neonatal hypercalcemia, and a set of facial and physical features that includes cardiovascular defects, typically congenital supravalvular aortic stenosis (Table 1; Morris, Leonard, & Dilates, 1988; Morris, Loker, Ensing, & Stock, 1993). However, what is most striking about individuals with WMS is their unique cognitive profile. The power of WMS as a model for dissecting cognition lies in the distinct pattern of abilities and deficits. Individuals with WMS perform relatively well on tasks involving language and face processing, but show extreme difficulties on other aspects of spatial processing and auditory processing, particularly at the level of global organization (Bellugi, Wang, & Jernigan, 1994; Bellugi, Klima, & Wang, 1996; Bellugi, Lichtenberger, Mills, Galaburda, & Korenberg, 1999a; Bellugi, Mills, Jernigan, Hickok, & Galaburda, 1999b; Bellugi, Lichtenberger, Jones, Lai, & St. George, this volume). WMS is also associated with hyperacusis, an abnormal sensitivity to sound (Neville et al., 1994), although this is not linked to abnormalities in the peripheral auditory system. Finally, the prime characteristic of WMS individuals is a strong impulse toward social contact and affective expression (Jones et al., this volume; Bellugi & Wang, 1998; Bellugi, Losh, Reilly, & Anderson, 1998; Bellugi et al., 1999a; Reilly, Klima, & Bellugi, 1990) as well as a heightened sensitivity to music (Levitin & Bellugi, 1998).

The neurobiological profile of WMS is being revealed through the studies of brain function, structure, and cytoarchitechtonics. In these domains, specific event-related potentials (ERPs) have been defined as markers for aspects of face and language processing in WMS (Mills et al., this volume; Bellugi et al., 1999b; Neville, Mills, & Bellugi, 1994). Neuroanatomical studies employing MRI and histomorphometric approaches have revealed consistent morphological features of decreased overall cerebral cortical volume; spared limbic structures of the temporal lobe including the amygdala, hippocampus, and parahippocampal gyrus; larger neocerebellar vs. paleocerebellar lobules (Jernigan & Bellugi, 1994); and preservation in volume of Heschl's gyrus, an area in the primary auditory cortex (Reiss et al., this volume; Bellugi et al., 1999b; Galaburda, Wang,

Table 1. Summary of Major WMS Phenotypic Features

Neurological	*Neurocognitive*	*Facies*
• Average IQ 55 (range 40-80)	• Friendly, loquacious personality	• Medial eyebrow flare
• Mild neurological dysfunction - Tight heel cords - Poor coordination	• Enhanced musical ability	• Short nasal palpebral fissures; epicanthal folds
• Hyperacussis	• Relatively spared language development, enhanced vocabulary, and social use of language compared to visual-spatial perception	• Flat nasal bridge
• Harsh, brassy or hoarse voice		• Stellate iris
		• Long philtrum
		• Prominent lips with open mouth

Cardiovascular	*Musculoskeletal*
• Supravalvular aortic stenosis	• Joint limitations
• Peripheral pulmonary artery stenosis	• Kyphoscoliosis
• Pulmonic valvular stenosis	• Hallux valgus
• Ventricular/atrial septal defects	• Hypoplastic nails
Genitourinary	*Endocrine*
• Nephrocalcinosis	• Transient infantile hypercalcemia
• Small, solitary, and/or pelvic kidneys	
• Vesicouretal reflux	

Bellugi, & Rossen, 1994; Galaburda & Bellugi, this volume). These features have been related to both the functional abnormalities and their possible embryological origins. Using the approach described, it is these neurocognitive and neurobiological features that will ultimately be combined with the genetic structure of WMS individuals to define the genes and pathways responsible.

Genetics of WMS

WMS is generally associated with a 1–2 Mb deletion of chromosome band 7q11.23 that includes the genes for elastin (Robinson et al., 1996; Gilbert-Dussardier et al., 1995; Nickerson, Greenberg, Keating, McCaskill, & Schaffer, 1995; Ewart et al., 1993), which is responsible for the congenital heart disease (Ewart, Jin, Atkinson, Morris, & Keating, 1994; Curran et al., 1993), LIM-kinase 1, which may contribute in part to the spatial deficit (Frangiskakis et al., 1996), and a growing number of other genes mapping in the region (illustrated in Figure 5). However, although WMS is clearly caused by the direct and downstream effects of genes located within the commonly deleted region, specific genes responsible for the major neurocognitive and physical features of WMS remain unknown. Gene candidates and transcripts mapping in the region include: *WSCR1–5* (Osborne et al., 1996); *RFC2*, the replication factor C subunit 2 (Peoples, Perez-Jurado, Wang, Kaplan, & Francke, 1996); *FZD9*, the human frizzled homolog of the *Drosophila wnt* receptor (Wang et al., 1997); *STX1A*, the syntaxin 1A gene (Osborne et al., 1997b); *GTF2I*, general transcription factor 2I (Perez-Jurado et al., 1998); WS-βTRP (WS-beta transducin repeats protein, ubiquitously expressed); *WS-bHLH* (a novel gene of the basic helix–loop–helix leucine zipper family of transcription factors that bind to E boxes, predominantly expressed in liver and kidney); *BCL7B*, a novel ubiquitously expressed gene (Meng et al., 1998); WSTF, WMS transcription factor (Lu, Meng, Morris, & Keating, 1998); FKBP6 (FK-506 binding protein, ubiquitously expressed); *CYLN2* (cytoplasmic linker-2 gene encoding the protein CLIP-115) (Hoogenraad et al., 1998); CPE-R (*Clostridium perfringens* enterotoxin receptor); and RVP1 (rat ventral prostate protein 1) (Paperna, Peoples, Wang, & Francke, 1998). In addition, the gene for NCF1 (neutrophil cytosolic factor 1) is located close to but is not deleted in WMS (Francke et al., 1990). It is not known which of these genes contributes to the phenotypic features of WMS. Using analyses of WMS subjects with atypical deletions, this report will illustrate the assignment of parts of the cognitive phenotype to the subsets of these genes.

Of importance for understanding both the cause and the phenotypic variability of WMS is the existence of genomic duplications that flank the largely unique region containing the genes described above. Both expressed genes and pseudogenes, as well as the breakpoints in the common WMS deletion, are thought to be located in these duplicated regions (Meng et al., 1998; Perez-Jurado et al., 1998; Osborne et al., 1997a; Korenberg et al., 1996; Robinson et al., 1996). However, the number of expressed genes in these duplicated regions and their contribution to the WMS phenotype is unknown. The current report will illustrate the structure of the flanking duplications and suggest a possible relationship to the WMS breakpoints.

In the current work, we will describe the construction of a working physical map of the WMS region including the flanking duplications. Combining data from fluorescence in situ hybridization (FISH), BAC end sequencing and large-scale sequence analyses, we will illustrate that the genomic organization of the WMS region includes two nested sets of duplications, the inner of which is involved in generating the common WMS deletion. A second gene for NCF1 will be shown to exist within the region deleted in some subjects with WMS. The genes for CPE-R and RVP1 have been assigned to single BACs. Three further gene fragments will be described and used to define the structure of the duplicated regions: *ATRA* (autoimmune thyroid antigen), a pseudogene for prohibitin that is located within an intron of the gene for GTF2I, and a novel gene that is duplicated but not deleted in WMS. Finally, using FISH and polymorphic marker analyses, we will describe the breakpoints in 78 individuals with WMS, two with larger deletions and one with a smaller deletion, and use this information to generate a phenotypic map of WMS, defining regions and genes likely to contribute independently to the mental retardation and to the facial features.

Data that describe progress in four areas will be presented below:

(a) The development of a physical map of the WMS region.
(b) Chromosomal breakpoints in WMS deletions.
(c) Evolution and human variation in the WMS region.
(d) The development of a phenotypic cognitive map of WMS.

RESULTS

The Development of a Physical Map of the WMS Region: Chromosome Band 7q11.23

Using an approach that is independent of previous maps, we have generated an array of bacterial artificial chromosomes (BACs) (Korenberg et al., 1996, 1999a, Korenberg, Lai, & Bellugi, 1999b; http://www.csmc.edu/genetics/korenberg/korenberg.html) covering the human genome at random, each mapped at 2–6 Mb resolution by using FISH (Korenberg & Chen, 1995;

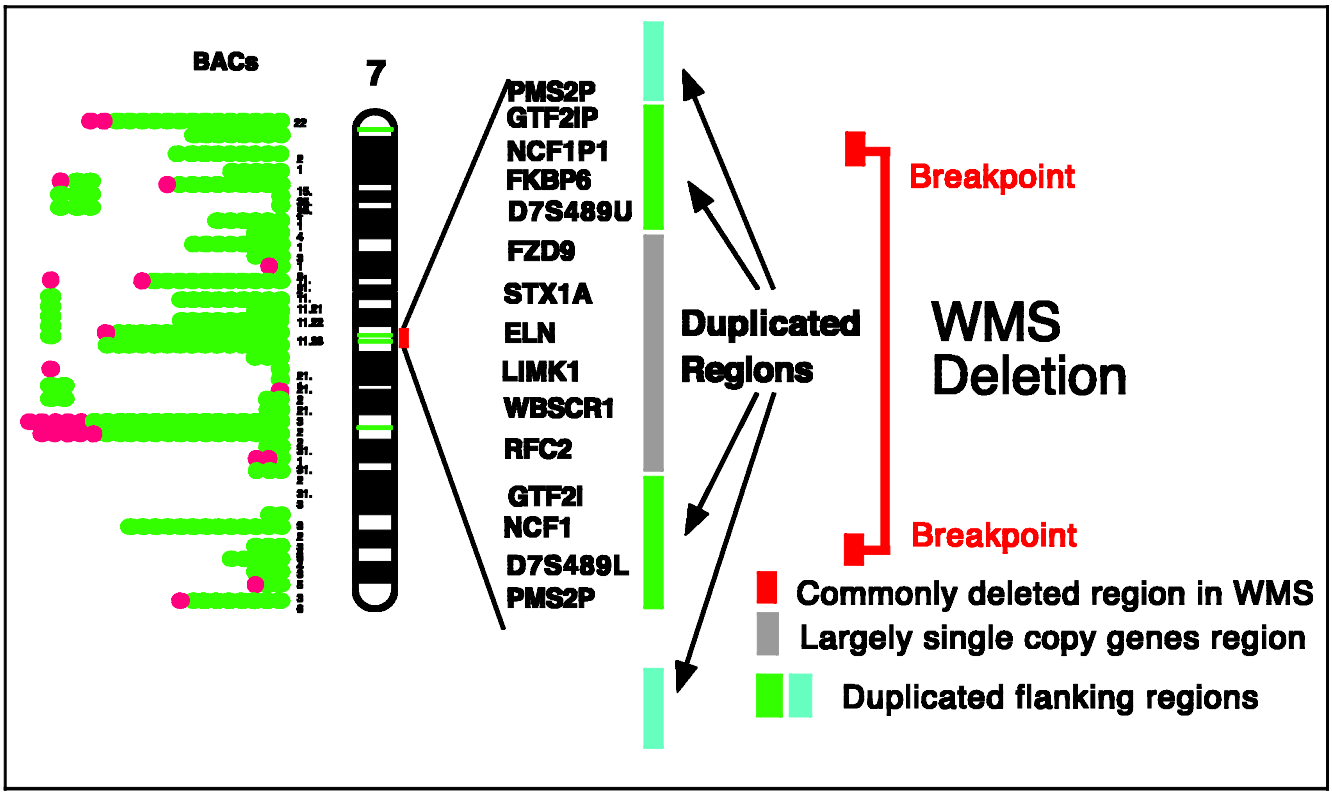

Figure 1. The region of chromosome 7, band 7q11.23, that is commonly deleted in WMS is represented by the red box in the ideogram. This region is expanded at the right to illustrate its genomic organization, a region of largely single-copy genes flanked by a series of genomic duplications (as indicated by bars) containing genes (e.g., *GTF2i*), pseudogenes (e.g., *GTF2I*, *PMS2P*), and duplicate markers (e.g., D7S489). The regions used in the common breakpoints are indicated by red bars. The map positions of independent BACs used in part for this analysis are shown as green dots to the left of the ideogram.

Korenberg, Chen, Adams, & Venter, 1995). A subset of these was used to construct a BAC array with which to investigate the WMS region of chromosome 7 (see Figure 1) because yeast artificial chromosome (YAC) arrays of this region were highly rearranged and deleted (http://www.genet.sickkids.on.ca/chromosome7). Forty-five of the initial 233 BACs mapping to chromosome 7 were located on band 7q11.2, of which 30 generated single and 15 generated large or clearly double signals along each of the sister chromatids within band 7q11.23, suggesting a local duplication within this band (Korenberg et al., 1996). A subset of these duplicated BACs also generated signals in band 7q22, suggesting the existence of sequences in 7q22 that were homologous to those in 7q11.23, extending previous reports of multiple pseudogene family members located in these bands (Nicolaides et al., 1995). PCR analyses revealed that BAC 592D8 carried the gene for elastin. To further establish the genomic organization of the region with respect to the elastin deletion associated with WMS, a series of three- and four-color FISH experiments was conducted on normal and WMS chromosome preparations. These experiments employed pairs of duplicated BACs that were hybridized simultaneously with single-copy BACs previously known to map within band 7q11.23. The results illustrated in Figure 1 indicated that BACs containing elastin (592D8 and 1148G3), and two further randomly defined BACs (155B1 and 363B4), defined a single-copy region that was flanked by two nested duplicated regions. The inner duplicated region was defined by sequences related to BAC 239C10 and more closely flanked elastin (Figure 2a and b). The outer duplicated region was defined by signals generated by BAC 611E3 (Figure 2c), that flanked the signals generated by BAC 239C10. This is shown in Figure 2d in which four-color interphase FISH analysis reveals BAC 592D8 surrounded by duplicate signals from BAC 239C10 that are in turn, flanked by duplicate signals generated by BAC 611E3. The interphase analyses of WMS subjects' chromosomes shown in Figure 2a, b, and d, revealed that the signals from the inner duplicated region appeared to fuse on the deleted chromosome (2b), whereas the outer layer of signals was not affected (2d). This suggested that the sequences identified by BAC 239C10 were close to or included in a common breakpoint responsible for the WMS deletion and is further discussed below.

The resulting model of layered duplications flanking a largely single-copy genomic region containing elastin is shown in Figures 1 and 3. It was inferred that this duplicated structure was likely predisposed

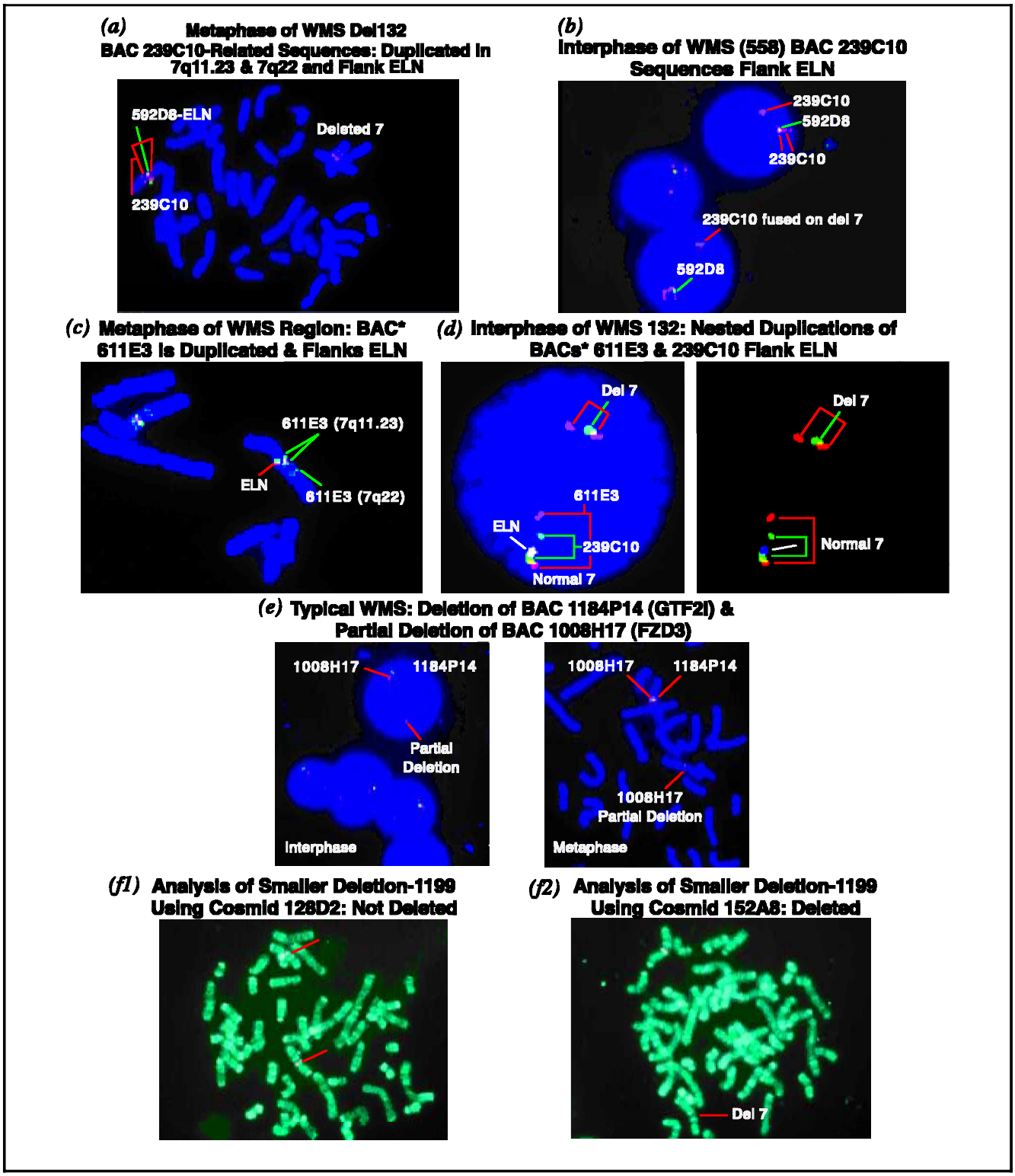

Figure 2. (**a** and **b**) BAC* indicates genomic sequences detected by and therefore presumed homologous to a given BAC. BAC* 239C10 (red) is duplicated within chromosome bands 7q11.23 as reflected by the large size of the signal on metaphase chromosomes (**a**), and signals are also seen in 7q22. As shown in the more extended DNA of interphase cells (**b**), BAC* 239C10 signals (red) flank the signals from BAC 592D8 (green) that carries the gene encoding elastin. (**c**) BAC* 611E3 (green) yields two clear signals within chromosome band 7q11.23, representing duplicated regions. The duplicated signals flank the single signal from BAC 592D8 (ELN) (red) as shown in metaphase chromosomes. (**d**) The duplicated signals from BAC 611E3 (red) surround those from BAC 239C10 (green) reflecting a nested duplication structure. Both signal sets flank the signal from BAC 592D8 (blue) as illustrated in these interphase cells. (**e**) BAC 1184P14 (green) carries the 5′ region of the gene encoding GTF2I and is shown to be deleted in subjects with the common WMS deletion. BAC 1008H17 (red) carries the gene encoding FZD9 and generates a small signal indicating partial deletion in subjects with the common WMS deletion. (**f1** and **f2**) Two cosmids detect different deletion patterns in WMS subject RM1199 with a smaller deletion. Cosmid 128D2 detects no deletion (**f1**), whereas cosmid 152A8 detects deletion (**f2**).

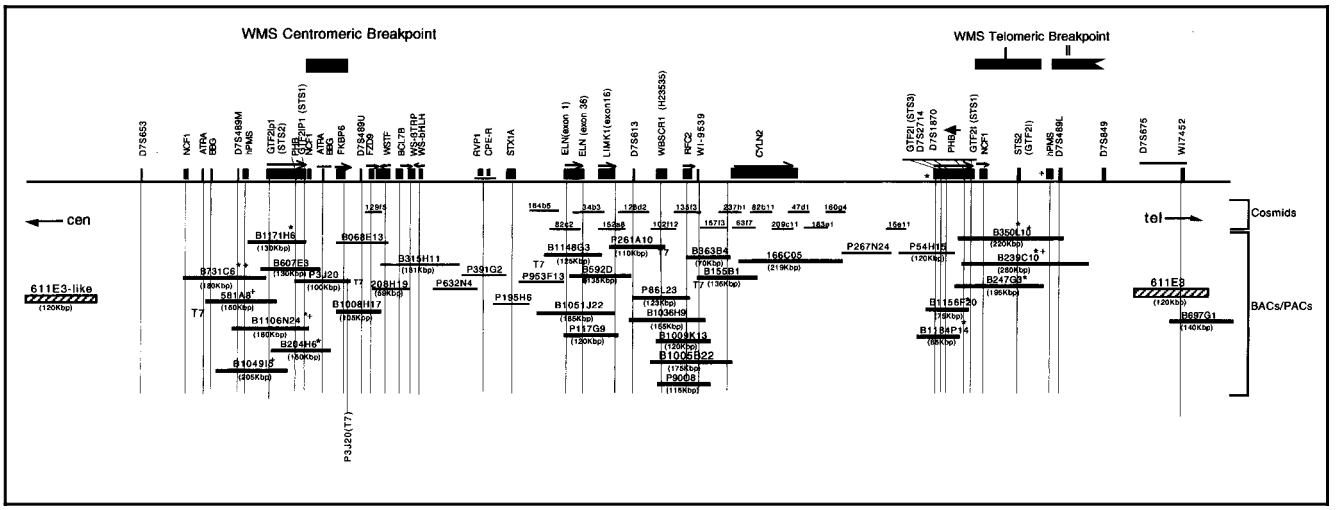

Figure 3. A physical and transcript map of the WMS region. Genes and pseudogenes mapping in this region are represented by black boxes (names reading vertically). BAC, PAC, and cosmid clones spanning this region are indicated below the genes and described in the Methods. The clones hybridized by using cDNA BAP135 are indicated by *, the clones hybridized by using cDNA PMS2 are indicated by +, and the clones of uncertain map position are indicated by ◇. The relative locations of genes, microsatellite markers, and clones was confirmed by using PCR analysis. The location of BAC 611E3 is indicated by the patterned box and is not linked to the remaining contiguous clones. The open box for CYLN2 indicates unknown location of the 3′ end.

to the deletion responsible for WMS by meiotic mispairing.

STS and Southern Analyses Order the Duplicated Regions and Identify Clones that Anchor the Unique to the Repeated Regions at the Inner Borders of the Duplications

The model and organization of the two duplicated regions was further investigated by the analysis of BACs recognizing duplicated regions. This employed BAC to BAC Southern blots; sizing by pulsed field gel analyses; PCR (see Methods for table) and Southern analyses of ordered polymorphic and STS linked markers and the products of cDNA selection; sequencing and analysis of BAC ends; and analysis of expressed sequence tags (ESTs) developed from sequencing BAC 239C10. Details of STS analyses including end sequences will be presented elsewhere. BAC to BAC Southern blots employed the 45 BAC DNAs mapping in 7q11.2 digested with *Eco*RI probed with whole BAC DNAs (BAC to BAC Southerns). These revealed cohybridization of BACs in the duplicated regions that confirmed the BAC groupings (239C10 related, 611E3 related, and closer relatedness of 607E3 with 731C6), than of all other BACs carrying the marker D7S489M, including 581A8, 1106N4, and 1049I5. BAC to BAC Southerns also indicated the overlap of BACs 363B4 and 155B1 in the single-copy region, the overlap of single-copy BAC 697G1 with duplicated BACs 611 E3. PCR analyses with single-site polymorphic markers shown on the map D7S489L(A), D7S489U(B), D7S489M(C) (Perez-Jurado et al., 1998; Osborne et al., 1996, 1997a; Robinson et al., 1996), permitted the assignment of BACs from the duplicated regions to the centromeric or telomeric side of the single-copy region as illustrated (Figure 3), with 239C10 location later confirmed by continuity of DNA sequence from telomeric markers and large-scale sequence of BAC 350L10. As a way of determining the correct overlap in such highly related regions, the sequencing of BAC ends was used to exclude or to confirm overlap but, because of the extensive sequence duplication and conservation within the duplicated region, was rarely useful for definitive overlap. Given the high sequence homology determined from initial BAC end sequencing, the overlap of BACs without anchored markers was determined by best fit of all analyses. BACs that are highly duplicated and without anchoring polymorphic markers remain without definitive map assignment and are indicated in the map by diamonds. For example, although STS analyses for BACs 1171H6, 607E3, and 247G3 were compatible with both centromeric and telomeric locations, BAC to BAC Southerns suggested location as shown in Figure 3. In summary, from FISH, DNA sequence, and genomic Southern data, the duplications flanking the WMS region appeared to consist of multiple regions of highly homologous DNA sequences.

Anchor clones were defined in a manner that linked the single-copy region to the flanking centromeric and telomeric duplicated regions. These were 1008H17 (centromeric), that was initially identified at random and by PCR, was then found to carry both duplicated D7489U(B) and single-copy sequences of FZD9, both of which are deleted in the common WMS deletion (Wang et al., 1997). Therefore, it was clear that both single-copy and duplicated sequences were deleted in the common deletion. Moreover, this established the clone (1008H17) as carrying sequences

that included the border of the single-copy and duplicated regions. FISH using this clone (1008H17 with FZD9) indicated that most individuals with WMS were partially deleted (Figure 2e). Further evidence supported this clone or the overlapping P1 artificial chromosome (PAC) 3J20 as containing the common breakpoint for the WMS deletion. This was suggested because PAC 3J20 carried both the commonly deleted marker D7489U and the nondeleted marker, *GTF2IP*, a pseudogene for the true gene, *GTF2I*, which is located at the telomeric end of the WMS common deletion (Perez-Jurado et al., 1998). Therefore, clones 1008H17 or 3J20 must contain the common centromeric breakpoint for WMS.

BAC clones anchoring the telomeric end of the single-copy region to the duplicated region, 1184P14 and 1156F20, were identified by screening for the unique marker D7S1870. These were found by BAC Southern analyses to carry a duplicated gene, initially called *BAP135* (data not shown), and then were confirmed to carry the 5′ STSs of the expressed form of the gene recently identified as *GTF2I* that is deleted in WMS (Perez-Jurado et al., 1998). This clone is deleted in all subjects with the common WMS deletion (Figure 2e), providing a reagent with which to define the telomeric end of the common WMS deletion.

Clone 611E3 May Anchor the Telomeric Duplicated Region to the Flanking Unique Region Located at the Border of Bands 7q11.23 and 7q21.1

The border between the telomeric duplicated region and the flanking single-copy region may be located close to or within BACs 611E3 or 697G1 since both carry the single-copy STS marker D7S2323, that is located telomeric to D7S489L, located in the telomeric duplication. BAC 697G1 is single copy (by FISH criteria) and maps by FISH to the border of bands 7q11.23-21. However, given the highly reduplicated nature of the entire region, the possibility remains that there are further duplicated regions flanking that defined by BAC611E3. Moreover, even the putatively single-copy STS, D7S2323, may itself be duplicated, and another copy of it located on the centromeric side of the WMS deleted region or in band 7q22. Nonetheless, these data suggest that there are regions in 7q11.23 that have been duplicated but are not involved in generating the WMS deletion.

Duplications Flanking the Elastin Region Contain Highly Conserved Gene Duplications and Processed Pseudogenes Originating from Many Chromosomes: Gene Sequences for NCF1, ATRA and Prohibitin are Duplicated in the Centromeric and Telomeric Regions Flanking the WMS Deletion

To further investigate duplicated genes and to establish their potential relationship to the WMS deletion and phenotype, BAC 239C10 was partially sequenced and, along with BAC end sequences, was analyzed by database comparisons using BLAST searches (Altschul et al., 1997). Previously known genes located in the single-copy deleted region (*ELN*, *LIMK1*, *WSCR1*, *RFC2*, *STX1A*, *FZD9*), in the putatively nondeleted (*NCF1* or neutrophil cytosolic factor 1), and in the duplicated regions (*PMS2*) were used to analyze all single and duplicated BACs by PCR, BAC Southern blots and sequence analyses of BAC 239C10. The gene for NCF1, previously mapped to 7q11.23 (Francke et al., 1990), but not thought deleted, was revealed to have at least three copies in the duplicated regions, two centromeric and one telomeric, by using a cDNA hybridized to BAC Southerns (data not shown). BAC 239C10 sequence analysis revealed a complete copy of the gene with a one-hundred-percent match to the published cDNA, and conservation of the appropriate intron/exon boundary sequences, located about 13 kb telomeric to the 3′ end of *GTF2I* and transcribed centromere to telomere. However, comparison of the genomic sequence containing this *NCF1* gene, with the genomic sequence of NCF1 that had been previously determined (Gorlach et al., 1997), revealed numerous changes within the introns. Therefore, this new copy of the *NCF1* gene, located in BAC 239C10, was considered to be an *NCF1* gene duplication and possibly expressed. The previously described copy of *NCF1* was inferred to be likely located in the centromeric duplication, defined by the previous genomic sequence (Gorlach et al., 1997). Nonetheless, differences within introns or in more extended regions at intron/exon boundaries may alter the likelihood of expression. No further sequences matching *NCF1* were found in BAC 239C10 or in the overlapping BAC 350L11. In summary, as begun above, further analyses of the regions flanking the common WMS deletion indicate long stretches of conserved and highly homologous DNA.

Sequence analysis of BAC 239C10 also revealed further genes or fragments located within the duplicated regions. For example, a one-hundred-percent match to all but the 5′ end of the gene *BAP135* (*GTF2I*) was found within the centromeric 9 kb, along with matches to other exons located in an unlinked 34 kb contig. It was shown to be duplicated by Southerns in at least one further copy on the centromeric duplication. Recent work (Perez-Jurado et al., 1998) has confirmed the locations of this gene, now renamed *GTF2I*, and its centromeric pseudogene, along with the intron/exon structure. STSs from these cDNAs, conserved at close to one hundred percent for all but the unique 5′ regions, were then used in the present analysis and are summarized in Figure 3. Further BAC 239C10 sequence analyses revealed the presence of a processed pseudogene for the prohibitin gene, containing numerous stop codons, and located at the centromeric end within intron 18 of *GTF2I* but transcribed in the opposite direction. The parent gene is located on chromosome 17q but PCR

analyses revealed that sequences related to this gene were duplicated on all BACs containing *GTF2I*. This suggests that the insertion of the prohibitin pseudogene predated the formation of the duplications flanking the WMS region, and the degree of sequence drift separating the functional and the pseudogenes might be used as a molecular clock to estimate the time since and evolutionary origin of the duplicated regions. Finally, the marker D7S489L was also confirmed to exist on BAC 239C10, as were pseudogenes for PMS2. Members of the PMS2 family of pseudogenes were previously known to be located in bands 7q11.2, 7p22, 7p13, and 7q22 (Nicolaides et al., 1995). The number of pseudogenes determined by PCR may underestimate the copy number determined by hybridization because of gene rearrangements or sequence drift. Nonetheless, because of their distribution (Korenberg, unpublished) the *PMS2* pseudogene family may provide an even more ancient tag than prohibitin for sequences that are ultimately responsible for the duplications flanking WMS.

Further gene fragments mapping in the duplicated regions were determined by end sequencing. For example, BAC 581A8 end sequence matched a gene fragment for ATRA (autoimmune thyroid disease-related antigen; M28639, Hirayu, Seto, Magnusson, Filetti, & Rapoport, 1987). Southern analyses revealed duplication as shown in Figure 2. Screening a brain cDNA library for the complete cDNA revealed an expressed pseudogene containing ATRA fused to a fragment from a novel gene isolated from a brain library (*BBG* in Figure 3) (Ishikawa et al., 1998) with both fragments located in multiple copies in the duplicated region. Further details will be reported elsewhere.

In order to determine the degree of homology and structure of the duplicated regions, Southern analyses were followed with sequencing of PCR fragments templated on BACs in the duplicated regions because, in most cases, identical fragment sizes were obtained from the Southern analyses. However, sequence analyses revealed a ninety-seven- to one-hundred-percent homology of sequences from BACs located on the two sides of the duplicated regions. The exceedingly high homology of some sequences flanking the WMS deleted region suggested either recent origin or a mechanism that selectively maintained homology; in either case, the high homology provides challenges to the genomic analysis and may predispose to mispairing at meiosis, thereby increasing variability genetic variability in this region.

Genes in the Single-Copy Region

To cover the single-copy region, PCR fragments from BAC end sequences (155B1, 363B4, 1184G3, 1008H17), mapped markers (D7S1870), and cDNA sequences (LIMK1, elastin) were used to screen the BAC library (Research Genetics, Huntsville, AL), followed by confirmation of overlap by PCR. The map of the single-copy region was further confirmed by PCR of genes and markers indicated on the map and was linked to other ordered clone sets (Meng et al., 1998a; Meng, Lu, Morris, & Keating, 1998b; Paperna et al., 1998; Osborne et al., 1997a, 1997b) by PCR and Southern analyses. The genes for CPE-R (*Clostridium perfringens* enterotoxin receptor) and RVP-1 (rat ventral prostate 1 protein), both recently mapped to the region between STX1A and FZD9 (Paperna et al., 1998), were mapped to PAC 391G2 by PCR. All putatively single-copy genes were evaluated for possible duplication by PCR and hybridization to BACs from the duplicated regions. Further cosmids and PACs obtained as indicated from other groups, were confirmed by PCR and Southerns to overlap as shown on the map in Figure 3.

The conclusion from these experiments was that the WMS region of band 7q11.2 was composed of a largely single-copy region of about 1.5 Mb containing at least 19 known genes. This region is flanked by duplications containing highly conserved processed and unprocessed pseudogenes, some of which are transcribed and many with homologies of ninety-nine percent. The next critical questions were to determine which of the single copy and which of the duplicated genes and pseudogenes were deleted in subjects with WMS and of these, which were important for determining the phenotype. To do this, the map reagents and information were then used to determine the regions and genes deleted in subjects diagnosed with WMS.

Chromosomal Breakpoints in WMS Deletions

The Inner Duplication is Involved in the WMS Common Deletion

Next, the BAC map reagents were used to determine the regions deleted in WMS subjects, to estimate the size of the deletion, and to define closely flanking markers. To do this, each of the 40 initial BACs randomly mapping in 7q11.2 was tested singly on metaphase and interphase chromosomes from six WMS subjects and evaluated with respect to the deleted chromosome using simultaneous hybridization of a control BAC located in band 7q22. The results illustrated in Figure 2 for BAC 239C10, clearly showed that the signals from BACs 239C10 and 731C6 that flanked elastin, were now joined in a single, smaller signal on the chromosome carrying the deletion whereas the duplicated signals from BAC 611E3, that flanked the 239C10 duplicated region now moved closer on the deleted chromosome but were not joined, as shown in Figure 2. BAC 731C6 generated smaller, more defined signals on interphase analyses. A third pattern was seen by BAC 204H6, which generated duplicated signals that were more diffuse and more closely surrounding the single-copy region (data not shown). These results suggested that the deletion breakpoints were located within or very close to the sequences

recognized by BAC 239C10 and that part of the duplicated region was itself deleted.

WMS Chromosomes Delete Parts of the Clones that Anchor the Unique and Duplicated Regions

To determine the regions commonly deleted in WMS, 74 subjects with clinically diagnosed WMS were tested as above. Chromosome preparations from subjects and 20 parents were analyzed by simultaneous FISH for BACs carrying elastin (592D8, 1051J22, 1148G3), the telomeric anchor clone that contained the gene for GTF2I, 1184P14; 239C10, and for 28 cases, the centromeric anchor BAC, 1008H17 (carrying the gene *FZD9*). The results summarized in Table 2, indicate that 73 of 74 subjects, but none of the parents (data not shown), were deleted for all single-copy BACs including the distal anchor marker. The common WMS deletion and the genes consequently deleted are shown in Figure 5. All save one were also partially deleted for the centromeric flanking marker 1008H17 and for BACs marking the flanking duplications (e.g., 239C10). The single case without a deletion was felt, on review, not to be typical, but, nonetheless, requires further study. This suggested that anchor BAC 1008H17 contained the centromeric breakpoint and that BAC 239C10 contained the telomeric breakpoint. Interphase analyses indicated that PAC 3J20 mapped on top of 1008H17, supporting it as the anchor and proximal breakpoint marker. The conclusion from this analysis was that the breakpoints of the common WMS deletion were not grossly variable but were rather clustered in a small region close to the centromeric and telomeric borders between the unique and repeated regions. This suggested that most subjects with WMS were deleted for roughly the same regions, and, therefore, variability in neurocognitive phenotype was not likely determined by large differences in gene content. It remained possible that genes at or near the breakpoints or within the duplicated regions, could contribute disproportionately to the classical WMS features. This spurred the search for rare subjects with smaller deletions.

Table 2. Summary: Analysis of Deletion in WMS Subjects Using FISH and Polymorphic Markers in Parents and Probands

Markers	*No. Deleted/ No. Subjects Tested*	*No. Deleted/ No. Informative*[a] (*n*= 112)	*Deleted (%)*
FISH with BACs			
FZD9 (B1008H17)	27/28		96.4
ELN+LIMK1 (B592D8)	73/74		98.6
RFC2 (B155B1)	8/8		100
GTF2I (B1184P14)	58/59		98.3
Microsatellites			
D7S653	34	0/25	0
D7S489U	36	9/9	100
D7S1870	39	26/26	100
D7S489L	34	2/11	18.2
D7S849	39	2/16	2.5
D7S675	38	0/25	0

[a]From ABI analysis.

WMS Subjects with Atypical Deletions

To further determine the extent of the deletions, particularly within the duplicated regions, microsatellite markers D7S489M, D7S489U, D7S1870, D7S489L, D7S849 (all except D7S489M, previously reported as deleted with variable frequencies), and the flanking markers, D7S675 and D7S653, were analyzed in parents and probands from 40 families. This revealed that 11 of the 40 probands were informative for D7S489L, and two of these 11 were deleted. All of the 26 informative probands were deleted for D7S1870, but not for the flanking markers (D7S675 and D7S653). A subset of phenotypic features for the two subjects with the atypical larger deletions are shown in Table 3 and the molecular data are shown in Figure 5. Both revealed typical WMS features. In addition, a further subject (data not shown), also carried a larger deletion and exhibited hyperlexia (ability to phonologically decode written words without necessarily comprehending them). Full neurocognitive analyses will be reported elsewhere (Korenberg et al., 1999a). In summary, the phenotypic features of WMS subjects with the common deletion or with the larger deletion are similar but may possess subtle neurocognitive differences that merit further study.

WMS subjects with smaller deletions were first identified by screening using FISH with the anchor BAC clones, 1184P14 and 1008H17, and BAC 592D8 (elastin) as reported elsewhere for Italian subjects, (Botta et al., 1999) and in a study of Japanese subjects. The clinical features of these along with those in the literature are shown in Table 3. One subject, RM1199, was found to be deleted for BAC 592D8 but for neither of the anchoring BACs. This 8-year-old girl had SVAS, a broad nasal tip, a slightly thick lower lip, dental anomalies, mild mental retardation, with a normal birth history. No further clinical information was available and photographs were not permitted. Further analyses employed the reagents from the map (Figure 3) for FISH (BACs 239C10, 315H11, 1148G3, 363B4, 155B1, PACs P632N4, 391G2, 195h6, 953F13, 261A10, 267N24, cosmids 129F5, 82C2, 152a8,

Table 3. Phenotypes of Eight Atypical WMS Subjects

Subject #	132	558	III1	III2	IV	V	VI	VII
Age at exam (Y)	11	13.3	6	2	13	7.8	19	29/26
Sex								
Male	•			•			•	•
Female		•	•		•	•		
Growth								
Weight %	95	7	97	3	40.5kg(46.0± 7.6)			
Height %	25	10	50	10	140.1cm(153.4± 5.6)	3– 10		
HC %	10		25	10		10		
Birth weight				low	2.6Kg	2.7Kg		
Physical features								
Face	+	+	+	+	±	–	–	– /–
Bulbous nasal tip/short	+/+	– /+	+/+	+	+	–	–	– /–
Lower lip thick	+	+	+	+/+	+	–	–	– /–
Malar flat	–	+	+	+	–	–	–	– /–
Periorbital fullness	–	+	+	+	–	–	–	– /–
Stellate iris	–	+	+		–	–	–	– /–
Epicanthal folds	+	+	+		–	–	–	– /–
Dental anomalies					+			
Hoarse voice	+	+			±	–	–	– /–
Heart								
SVAS	–	+	+		+	+	+	+/+
PA stenosis				+	–			
Renal anomalies					–	–	–	– /–
Hernia	–	+			–	–	–	+/+
Bony malformations								
Sloping shoulders	+	+			–	–	–	–
Long trunk	–	+			–	–	–	–
Neurological								
Abnormal gait	+	+			–	–	–	–
Cognitive								
Retardation								
Milestones retarded	+	+	+(mild)	+	+(mild)	normal	normal	n/n
IQ				68	54(65/51)	normal	normal	N range
Cognitive profile					±	–	–	–
Behavior								
Hypersocial	+	±	+		–			

128d2, 15e3, 183e1, 209c11, and 82b11), and quantitative Southern blot dosage analysis (data not shown) for the gene *FZD9*. The results (shown in Figure 2f and later in Figure 5) revealed the deletion of all contiguous clones from $B632N_4$ through cos152a8 but the presence of the overlapping anchor clones, B1008H17 and 129f5, indicating no apparent deletion of *FZD9* (confirmed by Southern analysis using gene-specific hybridization), but deletion for the remainder of the region including the genes telomeric to *FZD9*, viz., *STX1A*, *CPE-R*, *RVP1*, and *ELN*, and likely also for the genes, carried on the deleted BAC $B632N_4$. The telomeric breakpoint revealed deletion of clones through *LIMK1* but not for *WSCR1* or for sequences further telomeric. In summary, the analysis of WMS subject RM1199 revealed an atypical smaller deletion: Neither *FZD9* nor *GTF2I* were deleted, but the genes located telomeric to *FZD9* through *WBSCR1* were deleted.

The molecular data and subsets of the clinical and cognitive information from the subjects was then combined with data from the larger deletions described above, from other reports of individuals with SVAS and other features accompanied by deletion (Botta et al., 1999; Tassabehji et al., 1997, 1999; Frangiskakis et al., 1996; Olson et al., 1995) or single-base mutation of elastin (Li et al., 1997), and was used to generate a cognitive map as shown in Figure 5. This revealed regions likely to contain genes, which are in part responsible for the mental retardation and facial features, and, possibly, for a part of the hypersociability seen in WMS.

Evolution and Human Variation in the WMS Region

The duplicated region surrounding the WMS deletion can be traced through the evolution of primate chromosomes. This was investigated to better understand the origin of the duplicated regions and because of the possibility that changes in gene content and expression in the WMS region could be in part responsible for changes accompanying speciation in primates as well as for variation in human cognition. To do this, the chromosomal locations of BAC probes for the duplicated regions (239C10 and 611E3) and for the single-copy region (elastin, 592D8) were evaluated in the orangutan (*Pongo pygmaeus*), the gorilla (*Gorilla gorilla*), and the chimpanzee (*Pan troglodytes*). There have been two inversions in the higher primate homologues of human chromosome 7. The results, summarized in Figure 4, revealed that the region of 7q11.2 deleted in WMS has been involved in both of these evolutionary breakage and inversion events. The probes for both the duplicated and single-copy regions generated signals in the chromosome bands involved in the region of the

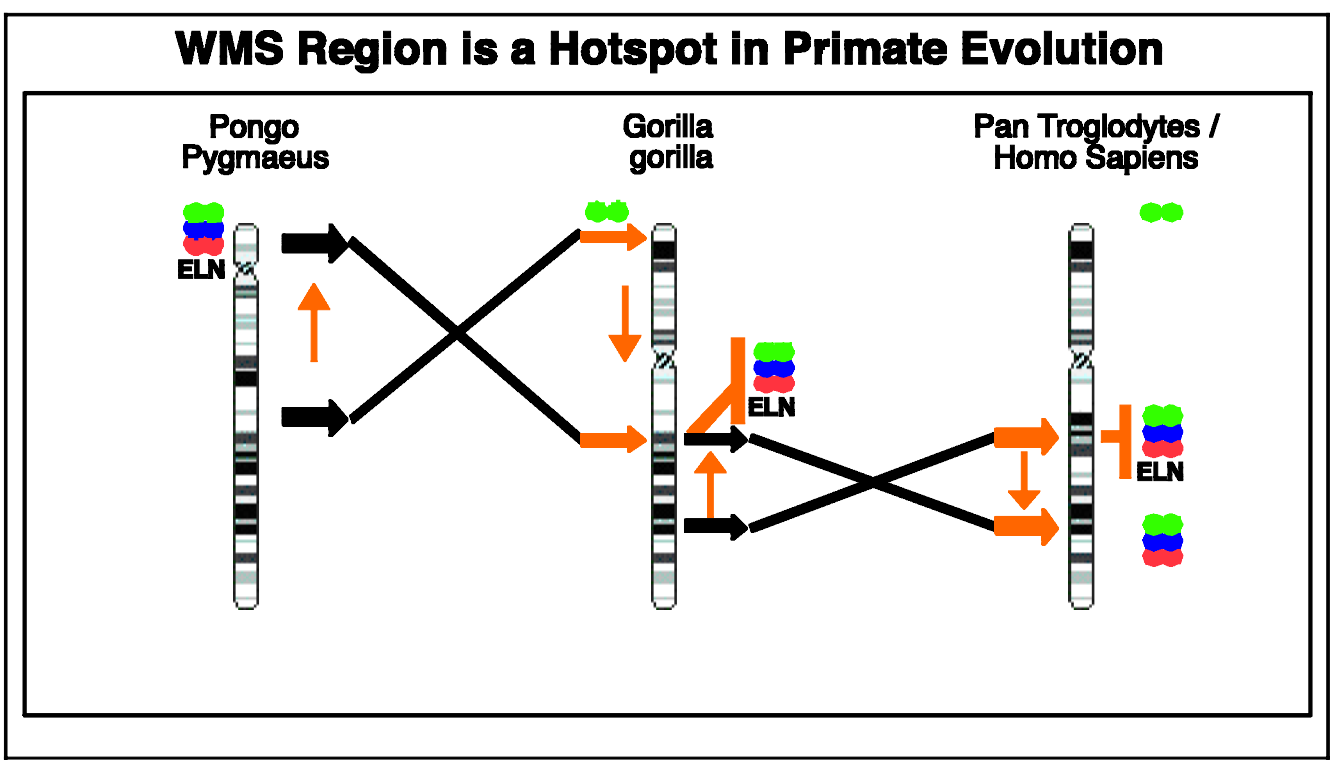

Figure 4. The human chromosome 7 homologs from the orangutan (*Pongo*), gorilla (*Gorilla*), and chimpanzee (*Pan*) are illustrated. Horizontal arrows indicate the approximate chromosome band of the major inversions that have accompanied their speciation. Experiments using BACs from the closely flanking duplicated regions (BACs 239C10, 204, and 611E3) for FISH revealed duplicated sequences located at or close to all inversion breakpoints, illustrated by the colored dots. The gene for elastin (*ELN*) mapped to the subtelomeric band of Pongo, and was close to the initial inversion breakpoint as well as all subsequent inversions of chromosome 7 through primate evolution.

inversions occurring between the orangutan and gorilla, and then again between the gorilla and the chimpanzee. It is of interest that the WMS region represented by BAC 239C10 was already partially duplicated in the orangutan, and appears to increase in signal with each inversion event, transferring part to the new site and leaving part of the duplicated region at the previous site, suggesting partial duplications associated with the inversions. The chimpanzee chromosome appears grossly similar in hybridization pattern to the human using the current probes but may vary for regions not yet tested. For all species changes, only the molecular analysis will allow an accurate understanding of the subtle rearrangements and potential duplications of these regions. Nonetheless, although such inversion and duplication is uncommon, it characterizes speciation during primate evolution. Therefore, we must ask to what extent these regions have contributed to primate speciation. Moreover, we must also ask whether humans are variable for these regions and for the expression of the genes within them, and to what extent might the normal variation of behavior in the cognitive domains we are looking at be determined by variation in these regions.

DISCUSSION

The physical map of the WMS region presented in this report reveals that the commonly deleted region is flanked by nested duplicated regions that are linked to the STS maps (see Figure 3). The inner duplicated region corresponds to the previously noted duplications that included PMS2, D7S489, and GTF2I (Perez-Jurado et al., 1998; Osborne et al., 1996). The current report extends the understanding of this region and suggests that the outer duplicated region appears asymmetrically located with respect to the gene for elastin. Moreover, the current analysis that is summarized in Figure 3 reveals that some subsections of the region are oriented in part in parallel and others are not. Further, the duplications themselves appear to be scrambled, somewhat reminiscent of the duplications found in chromosome band 5q13, in which deletion is responsible for SMA1 (Campbell, Potter, Ignatius, Dubowitz, & Davies, 1997). Moreover, some duplicated pseudogenes (*ATRA*, *BBG*, prohibitin) may also be located in band 7q22 (data not shown). All of this suggests that the formation of these regions included numerous events that occurred over an extended time period during primate or earlier evolution. Moreover, until the structure is supported by sequence data, it is still possible that the unit defined by D7489M is located in or duplicated in the telomeric duplication, and given the apparent multiple nature of the D7S489M signals, it is possible that there are further copies, and that the entire region is polymorphic in the human population. If D7S489M is duplicated, and at least one copy lies outside the deleted region, this would call into question its use in defining the usual WMS breakpoint. Finally, the genomic duplication of *NCF1* found in BAC 239C10 is of interest because the exon sequences are ninety-nine percent homologous to the putative functional copy located in the centromeric duplication but the intronic regions vary, being only ninety-seven percent homologous. This suggests that the telomeric duplication represented by BAC 239C10 is of recent origin, likely after the chimpanzee, or that the homology is maintained by some other mechanism, possibly gene conversion. Further, although this suggests that the gene for NCF1 was expressed for some time after duplication and may still be expressed by both the present telomeric and previously reported presumptively centromeric copies, this is made less likely by the observation of an autosomal recessive form of CGD (chronic granulomatous disease) that is caused by deletion of a GT in NCF1. The autosomal recessive inheritance implies that both parental copies, and, by inference, both centromeric and telomeric copies, would have to be mutated. Further analyses may yield differences in expressive potential due to promoter or intron/exon junction sequences.

Deletion Breakpoints in WMS: One Centromeric and At Least Two Telomeric

The definition of marker D7S849 as telomeric to D7S489L and possibly deleted in at least two individuals suggests the existence of a second telomeric breakpoint as indicated on the map in Figure 3. Although both the centromeric break and the first telomeric break appear to be common to most WMS deletions, by the current report as well as by previous analyses (Perez-Jurado et al., 1998; Robinson et al., 1996), further work is necessary to determine if the second break is also clustered. The second breakpoint may be located close to the outer ring of duplicated regions defined by BAC 611E3. It is of interest that we have placed a third *NCF1* copy close to the *GTF2I* pseudogene in the centromeric break and that these same genes appear to characterize the telomeric break, suggesting that sequences at or beyond the GTFZI 3′ and the 5′ end of *NCF1*, may be involved in the deletion as suggested (Perez-Jurado et al., 1998). It is important to note that the cause of the deletion may include a number of factors including the high frequency of Alu elements in the region and the high degree of sequence conservation in the duplicated regions. However, the limited localization of the breakpoints augers that particular sequences or chromatin structures may be major contributors. Candidate sequences could include any number of elements associated with genome instability (e.g., mariner elements, L1, HERV, THE1, etc.), although none of these have been demonstrated as causative. Finally, it is of interest

that BAC 611E3 may be located close to the 7q11.23-q21 border which delineates points at which stable replication forks must exist during DNA mitotic synthesis in that band q21 replicates late and band q11.23 earlier during the DNA synthetic period. The DNA structures that underlie the regions of band borders may themselves be unstable and may contribute to the tendency to delete.

We have, therefore, proposed that the repeat sequences illustrated by the BAC analyses are either responsible for or are caused by the same instabilities that lead to the deletion in WMS (Korenberg et al., 1997a, 1997b). In any event, it is likely that the meiotic mispairing of subsets of these sequence families combined with crossing-over (Robinson et al., 1996) results in a series of different chromosomal aberrations of the deletion/duplication types. Although these have not yet been described for the WMS region, similar duplicated structures on other chromosomes are also associated with deletions and rearrangements causing neurologic disease (Lupski, 1998). One fascinating aspect of this finding is the potential to define repeat sequence structures, and, therefore, other breakpoints and deletions that may be characteristic of particular phenotypes, adding another dimension to our understanding of genome organization and cognition.

Genes Responsible for Neurocognition, Neuroanatomy, and Behavior in WMS

The ultimate goal of this work was to understand the pathways that bridge genes and behavior by elucidating the genes deleted in different individuals with WMS, and by linking across levels, the information on gene expression, neuroanatomy, physiology, and neurocognition. To do this, we have presented the analysis of 74 subjects with clinically diagnosed WMS, which, together with other studies, has begun to show promise. The initial prospects for linking genotype and phenotype in WMS, with the traditional genetic approach, were grim since most all cases appeared to be deleted for the same region and the same genes (Perez-Jurado et al., 1998). Ideally, one would like to have seen some variability in the deletions and to link this with variations in cognitive behavior. Slowly, we are beginning to build up a database of these individuals who are partially deleted and show partial features of WMS. It is by combining the data from these subjects with other individuals carrying atypical deletions, that we have now begun to assign neurocognitive features of WMS to different regions with known genes.

The Development of a Phenotypic Cognitive Map of WMS

The result of combining the current molecular and cognitive data with the literature results in a suggestion of both the regions and the genes within that are ultimately involved in generating the phenotypic features of WMS. The current phenotypic map of WMS is shown in Figure 5.

The map was constructed by using the clinical data shown in Table 3 with the following rationale. In WMS, there is ample room for justifiable speculation as to which genes should be responsible for the cognitive features of WMS. The gene for LIMK1 has been implicated (Frangiskakis et al., 1996) but not substantiated (Tassabehji et al., 1999) as a cause of the visual–spatial features of WMS, and the genes for STX1A and FZD9 have been implicated simply by their brain-specific gene expression in the developing (FZD9) or adult (STX1A) central nervous system. However, regardless of the theoretical attraction of these molecules as mediators of cognitive processes and their embryological substrata, it is important to test their significance in causing the phenotypes at hand when they are underexpressed by fifty percent as is likely in the WMS brain. When this is done, as illustrated in Figure 5, we see that deletion of these genes is not associated with the significant effects on overall cognition that are characteristic of WMS. Therefore, we must now ask not only which genes are likely to affect cognition, but simultaneously, which regions and their genes have been demonstrated in humans to be associated with changes in cognition when deleted. First, it is now clear that deletion of elastin is responsible for the cardiovascular defects of WMS, based on the effects of both small deletions and point mutations of elastin. It is also strongly suggested that none of the other physical features is largely due to deletion of elastin. This is based on the lack of these features (e.g., facies, hoarse voice) in individuals with elastin single-base mutations (Li et al. 1997). Second, although a part of the visual–spatial deficit may be due to deletion of LIMK1 (Frangiskakis et al., 1996), this is unlikely to be the major gene responsible as the observation is not supported by three further cases that delete this gene as well as others (Tassabehji et al., 1999; Figure 4). The strength of this inference is emphasized by one of the cases being an engineering student. Third, from case RM1199 reported here, who is deleted for the region from WSTF through WSCR1, and the case CS (Tassabehji et al., 1999), who carries a deletion of the region from FZD9 through RFC2, it appears unlikely that the genes in this region can be largely responsible for the characteristic WMS mental retardation, sociability, visual–spatial or memory deficits, language preservation, or facial features. This is because both of these individuals have heart disease with essentially normal range or mildly impaired cognitive and physical features. Therefore, it is likely that the genes responsible for a major part of the mental retardation and other features are located in the region telomeric to *RFC2* through *GTF2I* at the telomeric border of the deletion. Nonetheless, the mild cognitive deficits seen in RM1199 and in one of the two subjects deleted for elastin and LIMK1 (Tassabehji

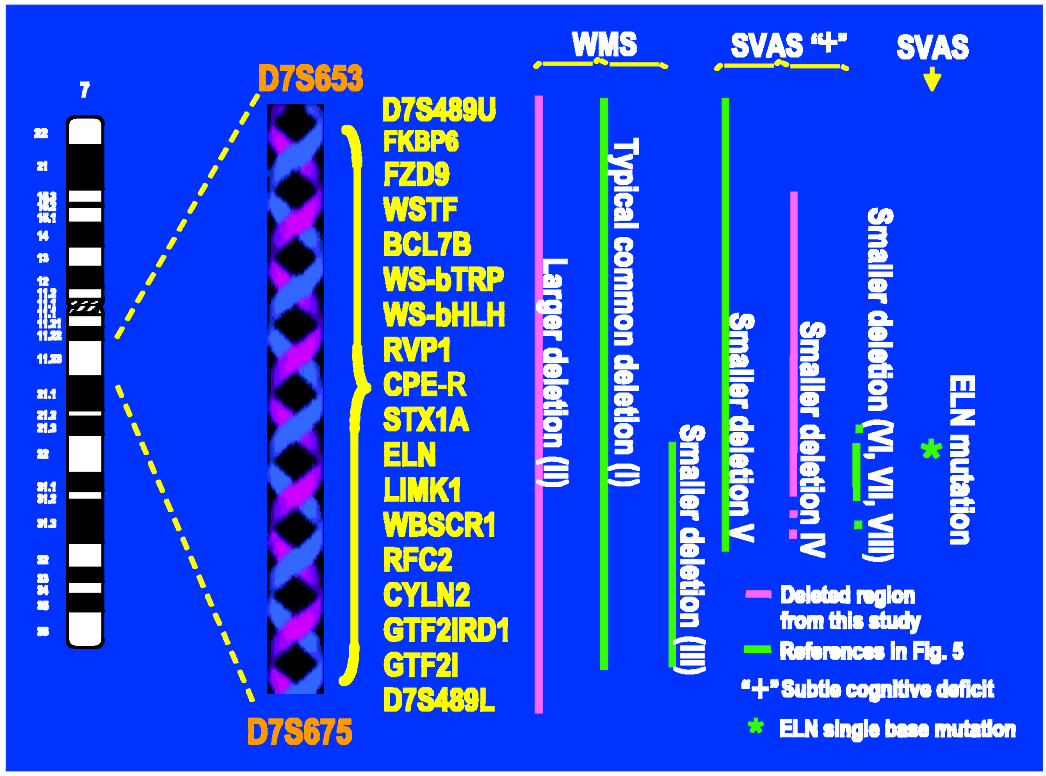

Figure 5. Vertical lines on both figures indicate the regions deleted, and the number of subjects carrying the common WMS deletion associated with some of the typical facial features, mental retardation, and heart disease, the larger deletion associated with similar features, or the smaller deletions, that include subregions of Synaxin1A through RFC2, associated with only the typical heart disease Supravalvar Aortic Stenosis (SVAS) and subtle cognitive deficits that fall within the normal range. Gene symbols are noted in the corresponding regions. Subject VIII has a subtle defect in visual–spatial processing. * Indicates individuals with deletion or single base pair mutation of elastin, all associated only with SVAS and normal cognition. Small vertical brackets indicate deleted regions that differ among subjects, and therefore provide the potential to assign specific WMS features to single regions or genes. Some brackets indicate regions that, from the current data, are likely to contain a gene or genes that when deleted contribute in some measure to the WMS features denoted. The significance of these data is that deletion of *STXIA*, *ELN*, *LIMK1*, *WSCR1*, and *RFC2* do not appear to be strongly associated with the characteristic facial or cognitive features seen in WMS, although they may contribute. In contrast, deletion of the region telomeric to *WSCR1* is associated with characteristic features of WMS cognition.

et al., 1999) suggest that decreased expression of genes in the region from WSTF through LIMK1 are associated with subtle defects in cognition. The contribution of genes in the telomeric region to the facial features and mental retardation is supported by the classical facial features seen in individuals with deletions of *STX1A* through *GTF2I* (Botta et al., 1999). Finally, it is important to note that, similar to subjects with the common full WMS deletion, the cognitive deficits in individuals with small deletions are variable and understanding the range of consequences of single deleted genes requires study of further individuals.

This exciting initial map of cognition is important in setting out the approach for defining the other domains of cognitive function and neuroanatomic structure as described above. Moreover, it emphasizes that, with a small number of subjects, however rare, significant understanding can be gained. From the map it is appreciated that, even with the small number of subjects currently reported, seven different regions could be defined for cognitive phenotypes that were delineated clearly. It is the development of sensitive measures and their study in these and other rare individuals that will ultimately provide clues to the critical steps in the pathways of human cognition.

Caveats to the WMS Cognitive Map

It is important to note that the variable expression of genes that are not deleted may also be affected and contribute to phenotype. These may include the effects of transcribed but not translated pseudogenes including those for GTF2I. Further sources of phenotypic variability include interactions of genes in the deleted region with others mapping both in and outside of the WMS region as well as possible regional disturbances of replication and transcription due to deletion and rearrangement. Such larger rearrangements that do not result in deletion may yet be a cause of the WMS phenotype by such a mechanism. Some rearrangements may lead to the decreased expression of nondeleted genes, and to the incorrect association of genes with

cognitive function. Ideally, gene expression in the brain both during fetal and adult life must be understood to assess this. However, the present map is a good beginning.

Other potential sources of genetic effects on cognition include imprinting, or the phenomenon by which the expression of a gene is differentially modified by passing through the maternal or the paternal germline. For WMS, this has been suggested for growth and head circumference (Pankau, Partsch, Neblung, Gosch, & Wessel, 1994; Francke, Yang-Feng, Brissenden, & Ulrich, 1986) and was recently investigated for a subset of the neurocognitive phenotypes (Korenberg et al., 1999). So far, it appears the parent of origin of the deletion is not related to the neurocognitive performance on any of the measures so far tested. These include overall intellectual ability, receptive and productive language, visual–spatial measures (with and without motor), and facial identification. However, other cognitive variables that have not yet been tested may be affected by the parent of origin. These may include memory (both verbal and visual, immediate, and long-term), conservation ability, frontal executive functions, friendliness and social behavior, and emotion perception. Although preliminary results indicated no significant difference, larger numbers of subjects and the development of more sensitive and specific measures may be required to elucidate more subtle effects of genetic imprinting on gene expression in WMS.

In summary, the data from studies of rare WMS subjects with atypical deletions are the most informative in identifying gene candidates for human cognitive features. Evidence suggests that mental retardation may be largely determined by the centromeric and telomeric regions and facial features determined at least in part determined by the telomeric region defined above. The next essential step is to parse the phenotype; to perform detailed cognitive, neuroanatomic, and physical studies of these individuals; and to devise and apply sensitive tests of musicality and sociability that probe the limits of these processes and that are informative across variation in intellectual function as seen in WMS. The multidimensional data from well-studied individuals with atypical deletions can thus be used to elucidate the many levels requiring intersection in the neurosciences; the role of neuroanatomic structures in cognition and behavior; and the role of gene expression in determining structure, cognition, and possibly disease.

METHODS

Clinical Subjects, DNA Isolation and Chromosome Preparation

Seventy-four WMS subjects used for this study were evaluated by the Laboratory for Cognitive Neuroscience at The Salk Institute for Biological Studies, La Jolla, CA. The procedures and consent forms were approved by The Salk Institute Institutional Review Board (IRB). DNAs were isolated either directly from peripheral blood or from lymphoblastoid cell lines using the Puregene DNA isolation Kit (Gentra, Minneapolis, MN) according to the manufacturer's instruction.

Chromosome preparations were generated by a standard technique from peripheral blood samples (Korenberg & Chen, 1995) for both humans and other primates. Primate bloods were obtained from the Yerkes Laboratory Yerkes Primate Research Institute/Emory University.

BAC to BAC Southerns

The BAC DNA preparations and the size of each clone were performed according to the procedure described by Hubert et al. (1997). Briefly, BAC DNAs were isolated using miniprep or midiprep kits (Qiagen) with modifications. *Not*I digests excised the insert and provided a convenient means of determining the sizes of clones. Southern blots of *Not*I and *Eco*RI double-digests of miniprep or midiprep DNA were used to show overlaps between clones. To prepare probes from BACs, 50–100 ng of DNAs were labeled using random priming (Boehringer Manheim). The hybridization and wash conditions were as described previously (Korenberg et al., 1995).

FISH and Chromosomal Analysis

The BAC clones were confirmed and mapped to chromosome 7q by using multicolor FISH as described previously (Korenberg et al., 1995). One microgram of miniprep BAC DNA was either indirectly labeled with biotin-14-dUTP or digoxigenin-11-dUTP or directly labeled with Cy5-dUTP, Arcour-dUTP using nicktranslation kits (GIBCO BRL; Amersham). FITC–avidin (Vector Lab) and Rhodamine–antidigoxigenin (Boehringer Manheim) were used for the detection of biotinylated and digoxigenin labeled probes, respectively. The directly labeled probes were viewed immediately after the counterstaining with chromomycin A3 and distamycin A, which generates a high-resolution reverse banded pattern. The color images were captured by using the Photometrics cooled-CCD camera and BDS image analysis software (ONCOR Imaging, Gaithersburg, MD).

To determine whether a given individual carried a deletion, BAC probes for elastin (592D8) were hybridized simultaneously with one or both anchor BACs (1184P14 carrying D7S1870 and 1008H17 carrying FZD9) as well as BAC 239C10 recognizing the flanking duplications. More than 20 cells of high technical quality were evaluated for each individual and scored for presence, absence or intermediate signal from each probe on both chromosomes. Deletions were scored only when all 20 cells revealed absent signals.

PCR Table

Genes	Access number/ref	5′ Primer sequences	3′ Primer sequences	PCR fragment sizes (bp)
NCF1	U57835	GGCCCCGCTCTCTGCCCGCA	GCAAGGGCCGAGACGCTAGC	182
FKBP6 exon 9	Meng et al., 1998			
WSTF exon 20	Lu et al., 1998			
FZD9	U82169	TGTCAAGGTCAGGCAAGTGAG	CTCACCTCCTACCTTCCCCCTTCCCAGCCA	283
CPE-R	AB000712	CTTCAGCCCAGGGCCCCTGG	GCACAGGTCCCATTTATTGT	224
RVP1	BA000714	GCATGGACTGTGAAACCTCA	GCTAAAACGAGAGGCTTTTA	170
STX1A	U87315	CCTGTTGTCTTGCGCTCTGGG	AGATACAAATGTTTATTCTAC	426
ELN exon 1	J02948	ATGGCGGGTCTGACGGCGGCG	GGATCCCGCTTCCCAGGGGTC	568
ELN exon 36	J02948	GGACTCACAGTGATGTGCACC	GGCGGCCATGACAGGTCAACC	828
LIMK1	U62292	CTTTGTGAAGCTGGAACACTGG	GTTCCTTGGACGTCACGGTTCC	1334
D7S613	G18333			
WSCR1	AF045555	AGCACAGAGACCACGACTCC	CTGCGTCAGCGCCGCAGTCA	160
H23535	G25613			
RFC2	AF045555	CCACTCGCCCACCCTCACGT	GCAGCTCACTAGGACATTCA	640
GTF2i-STS1, STS2, STS3	Perez-Jurado et al., 1998			
D7S1870	Z51768			
D7S489	z16646			
WI-9539	G11821			

PCR Analysis

All PCR primers were constructed as referenced or designed manually as shown in the Table. PCR reactions carried out in a PTC-100TM (MJ Research). PCRs were performed in 25–l reaction mixtures containing 0.5–1 M each primer and 0.5–1 U Taq in 10× PCR buffer and 25 µm each of dATP, dCTP, dTTP, dGTP (GIBCO BRL) with 1.5 mM $MgC1_2$. After initial denaturation (94°C for 2 min) and amplification for 30 cycles (94°C for 45 sec, 57°C for 60 sec, final extension 72°C for 10 min), products were resolved by gel electrophoresis on 1–3% ethidium brodide-stained NuSieve agarose gels.

Sequence Analysis

Sequencing the ends of BAC and PAC inserts directly: Sequencing primers that immediately flank the insert were designed from the SP6 and T7 RNA promoters and other sites within the vectors and were used to sequence BAC and PAC ends directly without subcloning. The primer sequences used were SP6, 5′ gatttaggtgacactgtag 3′, and T7, 5′ taatacgactcactataggg 3′. The sequencing reactions were performed as described in the dsDNA Cycle Sequencing System (BRL) using 6 g of midiprep DNA for each SP6 and T7 reaction. Electrophoresis in 60-cm, six-percent denaturing polyacrylamide gels gave up to 350 bp of sequence at 55W.

The University of Oklahoma's Advanced Center for Genome Technology (ACGT) (http://www.genome.ou.edu/human.html, AC004166) produced the large-scale sequencing of BAC clone 239C10. DNA sequence for BAC 350L10 was obtained from the Washington University Genome sequencing Center, as a series of unlinked contigs available at http//genome.wustl.edu/pub/gscl/sequence/st.louis/human/preliminary/7. The sequence of ATRA (EST M28639) and BBG were obtained by using BLAST search in NCBI database with the end sequence of BAC 581A8 (http://www.ncbi.nih.gov).

Genes and Markers

Cosmids 129F5, 165B5, 82C2, 34B3, 128D2, 102F12, 135F3, 157F3, 237H1, 63F7, 82B11, 209C11, 47D1,

183E1, 160G4, and 15E11 were a generous gift from Lap-Chee Tsui (Osborne et al., 1997a, 1997b). The information for DNA markers of D7489M, D7489U, D7489L, STS1, STS2, STS3, D7S2714, and D7S1870 were obtained either from the literature or the MIT web site (Perez-Jurado et al., 1998; Osborne et al., 1996; Gilbert-Dussardier et al., 1995) (http://www-genome.wi.mit.edu/).

Polymorphic Marker Analyses

Microsatellite analyses were conducted using D7S489(A,B,C), D7S1870, D7S653, D7S675, D7S849, D7S613, D7S2472, D7S2476. Primers were designed from publicly available sequences and labeled with one of the three following dyes: 6-Carboxyfluorescein, 6-carboxy-2′,4′,7′,4,7-hexachlorofluorescein, and *N*,*N*,*N*′,*N*′-tetramethyl-6-carboxyrhodamine. A fourth dye 6-carboxy-X-rhodamine labeled the lambda phage size standard. Multiplex PCR reactions were carried out in solutions containing 10 mM Tris–HCl (pH 8.9), 50 mM KCl, 2.5 mM $MgCl_2$, 100 ng genomic DNA, 200 μM from each subject.

Acknowledgments

This work was performed at Share's Child Disability Center and supported by grants from the Department of Energy (DE-PG03-92ER-61402 and DE-FC03-96ER62294 to J. R. Korenberg) and the National Institute of Child Health and Human Development (HD33113, J. R. Korenberg). J. R. Korenberg holds the Geri and Richard Brawerman Chair in Molecular Genetics. The work was also supported partially by grant NHGIN HG00313 to B. Roe and grants from The Oak Tree Philanthropic Foundation, and Call Foundation to U. Bellugi, and the James S. McDonnell Foundation to U. Bellugi and J. R. Korenberg.

Reprint requests should be sent to J. R. Korenberg, Medical Genetics, Cedars-Sinai Medical Center, 110 George Burns Road, Davis Building, Suite 2069, Los Angeles, CA 90048-1869, USA, or via e-mail: julie.korenberg@cshs.org.

REFERENCES

Altschul, S. F., Madden, T., Schaffer, A., Zhang, J., Zhang, H., Miller, W., & Lipman, D. J. (1997). Gapped BLAST and PSI-BLAST: A new generation of protein database search programs. *Nucleic Acids Research, 25,* 3389–3402.

Bellugi, U., Klima, E. S., & Wang, P. P. (1996). Cognitive and neural development: Clues from genetically based syndromes. In D. Magnussen (Ed.), *The life-span development of individuals: Behavioral, neurobiological, and psychosocial perspectives* (pp. 223–243). The Nobel Symposium. New York: Cambridge University Press.

Bellugi, U., Lichtenberger, L., Jones, W., Lai, Z., & St. George, M. (this volume). The neurocognitive profile of Williams Syndrome: A complex pattern of strengths and weaknesses.

Bellugi, U., Lichtenberger, L., Mills, D., Galaburda, A., & Korenberg, J. (1999a). Bridging cognition, brain and molecular genetics: Evidence from Williams syndrome. *Trends in Neurosciences, 22*, 197–207.

Bellugi, U., Losh, M., Reilly, J., & Anderson, D. (1998). Excessive use of linguistically encoded affect: Stories from young children with Williams syndrome (Technical Report CND-9801). University of California, San Diego, Center for Research in Language, Project in Cognitive and Neural Development.

Bellugi, U., Mills, D., Jernigan, T., Hickok, G., & Galaburda, A. (1999b). Linking cognition, brain structure and brain function in Williams syndrome. In H. Tager-Flusberg (Ed.), *Neurodevelopmental disorders: Contributions to a new framework from the cognitive neurosciences.* (pp. 111–136). Cambridge, MA: MIT Press.

Bellugi, U., & Wang, P. P. (1998). Williams syndrome: From cognition to brain to gene. In G. Edelman & B.H. Smith (Eds.), *Encyclopedia of Neuroscience*, CD-ROM version. New York: Elsevier.

Bellugi, U., Wang, P. P., & Jernigan, T. L. (1994). Williams syndrome: An unusual neuropsychological profile. In S. Broman & J. Grafman (Eds.), *Atypical cognitive deficits in developmental disorders: Implications for brain function* (pp. 23–56). Hillsdale, NJ: Erlbaum.

Botta, A., Novelli, G., Mari, A., Novelli, A., Sabani, M., Korenberg, J. R., Osborne, L., Digilio, M. C., Giannotti, A., & Dallapiccola, B. (1999). Detection of an atypical 7q11.23 deletion in Williams syndrome patients which does not include the STX1A and FZD9 genes. *Journal of Medical Genetics, 36,* 478–480.

Campbell, L., Potter, A., Ignatius, J., Dubowitz, V., & Davies, K. (1997). Genomic variation and gene conversion in spinal muscular atrophy: Implications for disease process and clinical phenotype. *American Journal of Human Genetics, 61,* 40–50.

Curran, M. E., Atkinson, D. L., Ewart, A. K., Morris, C. A., Leppert, M. F., & Keating M. T. (1993). The elastin gene is disrupted by a translocation associated with supravalvular aortic stenosis. *Cell, 73,* 159–168.

Ewart, A. K., Jin, W., Atkinson, D. L., Morris, C. A., & Keating, M. T. (1994). Supravalvular aortic stenosis associated with a deletion disrupting the elastin gene. *Journal of Clinical Investigations, 83,* 1071–1077.

Ewart, A. K., Morris, C. A., Atkinson, D., Jin, W., Sternes, K., Spallone, P., Stock, A. D., Leppert, M., & Keating, M. T. (1993). Hemizygosity at the elastin locus in the developmental disorder, Williams syndrome. *Nature Genetics, 5,* 11–18.

Francke, U., Hsieh, C. L., Foellmer, B. E., Lomax, K. J., Malech, H. L., & Leto, T. L. (1990). Genes for two autosomal recessive forms of chronic granulomatous disease assigned to 1q25 (NCF2) and 7q11.23 (NCF1). *American Journal of Human Genetics, 47,* 483–492.

Francke, U., Yang-Feng, T. L., Brissenden, J. E., & Ulrich, A. (1986). Chromosomal mapping of genes involved in growth control. *Cold Spring Harbor Symposium on Quantitative Biology, 51,* 855–866.

Frangiskakis, J. M., Ewart, A. K., Morris, C. A., Mervis, C. B., Bertrand, J., Robinson, B. F., Klein, B. P., Ensing, G. J., Everett, L. A., Green, E. D., Proschel, C., Gutowski, N. J., Noble, M., Atkinson, D. L., Odelberg, S. J., & Keating, M. T. (1996). LIM-kinase hemizygosity implicated in impaired visuospatial constructive cognition. *Cell, 86,* 59–69.

Galaburda, A., & Bellugi, U. (this volume). Multi-level analysis of cortical neuroanatomy in Williams syndrome.

Galaburda, A. M., Wang, P. P., Bellugi, U., & Rossen, M. (1994). Cytoarchitectonic findings in a genetically based disorder: Williams syndrome. *NeuroReport, 5,* 758–787.

Gilbert-Dussardier, B., Bonneau, D., Gigaral, N., Le Merrer, M., Bonnet, D., Phillip, N., Serville, F., Verloes, A., Rossi, A., Ayme, S., Weissenbach, J., Mattei, M.-G., Lyonnet, S., & Munnich, A. (1995). A novel microsatellite DNA marker at

locus D7S1870 detects hemizygosity in 75% of patients with Williams syndrome. *American Journal of Human Genetics, 56,* 542–543.

Gorlach, A., Lee, P. L., Roesler, J., Hopkins, P. J., Christensen, B., Green, E. D., Chanock, S. J., & Curnutte, J. T. (1997). A p47-phox pseudogene carries the most common mutation causing p47-phox-deficient chronic granulomatous disease. *Journal of Clinical Investigations, 100,* 1907–1918.

Hirayu, H., Seto, P., Magnusson, R. P., Filetti, S., & Rapoport, B. (1987). Molecular cloning and partial characterization of a new autoimmune thyroid disease-related antigen. *Journal of Clinical Endocrinology and Metabolism, 64,* 578–584.

Hoogenraad, C. C., Eussen, B. H., Langeveld, A., Haperen, R., Winterberg, S., Wouters, C. H., Grosveld, F., De Zeeuw, C. L., & Galjart, N. (1998). The murine CYLN2 gene: Genomic organization, chromosome localization and comparison to the human gene that is located within the 7q11.23 Williams syndrome critical region. *Genomics, 53,* 348–358.

Hubert, R. S., Mitchell, S., Chen, X.-N., Ekmekji, K., Gadomski, C., Sun, Z., Noya, D., Kim, U.-J., Chen, C., Shizuya, H., Simon, M., de Jong, P. J., & Korenberg, J. R. (1997). BAC and PAC contigs covering 3.5 Mb of the Down syndrome congenital heart disease region between D21S55 and MX1 on chromosome 21. *Genomics, 41,* 218–226.

Ishikawa, K., Nagase, T., Suyama, M., Tanaka, A., Kotani, H., Nomura, N., & Ohara, O. (1998). Prediction of the coding sequences of unidentified human genes: X. The complete sequences of 100 new cDNA clones from brain which can code for large proteins. *DNA Research, 176,* 169–176.

Jernigan, T. L., & Bellugi, U. (1994). Neuroanatomical distinctions between Williams and Down syndromes. In S. Broman and J. Grafman (Eds.), *Atypical cognitive deficits in developmental disorders: Implications in brain function* (pp. 57–66). Hillsdale, NJ: Erlbaum.

Jones, W., Bellugi, U., Lai, Z., Chiles, M., Reilly, J., Lincoln, A., & Adolphs, R. (this volume). Hypersociability in Williams syndrome.

Korenberg, J. R., & Chen, X.-N. (1995). Localization of human CREBBP (CREB Binding Protein) to 16p13.3 by fluorescence in situ hybridization. *Cytogenetics and Cell Genetics, 71,* 56–57.

Korenberg, J. R., Chen, X.-N., Adams, M.D., & Venter, J. C. (1995). Towards a cDNA map of the human genome. *Genomics, 29,* 364–370.

Korenberg, J. R., Chen, X.-N., Lai, Z., Yimlamai, D., Bisighini, R., & Bellugi, U. (1997a). Williams syndrome. The search for genetic origins of cognition. *American Journal of Human Genetics, 61,* A103, 579.

Korenberg, J. R., Chen, X.-N., Mitchell, S., Sun, Z.-G., Hubert, R., Vataru, E. S., & Bellugi, U. (1996). The genomic organization of Williams syndrome. *American Journal of Medical Genetics Supplement, 59,* A306, 1776.

Korenberg, J. R., Chen, X.-N., Mitchell, S., Sun, Z.-G., Hubert, R., Vataru, E. S., & Bellugi, U. (1997b). The genomic organization of Williams syndrome. *International Behavioral Neuroscience Society Abstracts, 6,* 59, P2-52.

Korenberg, J. R., Chen, X.-N., Sun, Z., Shi, Z.-Y., Ma, S., Vataru, E., Yimlamai, D., Weissenbach, J. S., Shizuya, H., Simon, M. I., Gerety, S. S., Nguyen, H., Zemsteva, I. S., Hui, L., Silva, J., Wu, X., Birren, B., & Hudson, T. J. (1999a). Human genome anatomy: BACs integrating the genetic and cytogenetic maps for bridging genome and biomedicine. *Genome Research, 9* (in press).

Korenberg, J. R., Lai, Z., & Bellugi, U. (1999b). In preparation.

Levitin, D. J., & Bellugi, U. (1998). Musical abilities in individuals with Williams syndrome. *Music Perception, 15,* 357–389.

Li, D. Y, Toland, A. E., Boak, B. B., Atkinson, D. L., Ensing, G. J., Morris, C. A., Keating, M. T. (1997). Elastin point mutations cause an obstructive vascular disease, supravalvular aortic stenosis. *Human Molecular Genetics, 6,* 1021–1028.

Lu, X., Meng, X., Morris, C. A., & Keating, M. T. (1998). A novel human gene, WSTF, is deleted in Williams syndrome. *Genomics, 54,* 241–249.

Lupski, J. R. (1998). Genomic disorders: Structural features of the genome can lead to DNA rearrangements and human disease traits. *Trends in Genetics, 10,* 417–422.

Meng, X., Lu, X., Li, Z., Green, E. D., Massa, H., Trask, B. J., Morris, C. A., & Keating, M. T. (1998a). Complete physical map of the common deletion region in Williams syndrome and identification and characterization of three novel genes. *Human Genetics, 103,* 590–599.

Meng, X., Lu, X., Morris, C. A., & Keating, M. T. (1998b). A novel human gene FKPB6 is deleted in Williams syndrome. *Genomics, 52,* 130–137.

Mills, D., Alvarez, T., St. George, M., Appelbaum, L., Bellugi, U., & Neville, H. J. (this volume). Electrophysiological studies of face processing in Williams syndrome.

Morris, C. A., Leonard, C. O., & Dilates, C. (1988). Natural history of Williams syndrome: Physical characteristics. *Journal of Pediatrics, 113,* 318–325.

Morris, C. A., Loker, J., Ensing, G., & Stock, A. D. (1993). Supravalvular aortic stenosis cosegregates with familial 6; 7 translocation which disrupts the elastin gene. *American Journal of Medical Genetics, 46,* 737–744.

Neville, H. J., Mills, D., & Bellugi, U. (1994). Effects of altered auditory sensitivity and age of language acquisition on the development of language-relevant neural systems: Preliminary studies of Williams syndrome. In S. Broman & J. Grafman (Eds.), *Atypical cognitive deficits in developmental disorders: Implications for brain function* (pp. 67–83). Hillsdale, NJ: Erlbaum.

Nickerson, E., Greenberg, F., Keating, M. T., McCaskill, C., & Shaffer, L. G. (1995). Deletions of the elastin gene at 7q11.23 occur in approximately 90% of patients with Williams syndrome. *American Journal of Human Genetics, 56,* 1156–1161.

Nicolaides, N. C., Carter, K., Shell, B. K., Papadopoulos, N., Vogelstein, B., & Kinzler, K. W. (1995). Genomic organization of the human PMS2 gene family. *Genomics, 30,* 195–206.

Olson, T. M., Michels, V. V., Urban, Z., Csiszar, K., Christiano, A. M., Driscoll, D. J., Feldt, R. H., Boyd, C. D., Thibodeau, S. N. (1995). A 30 kb deletion within the elastin gene results in familial supravalvular aortic stenosis. *Human Molecular Genetics, 4,* 1677–1679.

Osborne, L. R., Herbrick, J. A., Greavette, T., Heng, H. H., Tsui, L.-C., & Scherer, S.W. (1997a). PMS2-related genes flank the rearrangement breakpoints associated with Williams syndrome and other diseases on human chromosome 7. *Genomics, 45,* 402–406.

Osborne, L. R., Martindale, D., Scherer, S. W., Shi, X. M., Huizenga, J., Heng, H. H. Q., Costa, T., Pober, B., Lew, L., Brinkman, J., Rommens, J., Koop, B., & Tsui, L.-C. (1996). Identification of genes from a 500-kb region at 7q11.23 that is commonly deleted in Williams syndrome patients. *Genomics, 36,* 328–336.

Osborne, L. R., Sodar, S., Shi, X.-M., Pober, B., Costa, T., Scherer, S. W., & Tsui, L.-C. (1997b). Hemizygous deletion of the syntaxin 1A gene in individuals with Williams syndrome. *American Journal of Human Genetics, 61,* 449–452.

Pankau, R., Partsch, D. J., Neblung, A., Gosch, A., & Wessel, A. (1994). Head circumference of chidren with Williams–Beuren Syndrome. *American Journal of Medical Genetics, 52,* 285 –290.

Paperna, T., Peoples, R., Wang, Y. K., & Francke, U. (1998). Genes for the CPE receptor ($CPETR_1$) and the human homolog of RUP_1 ($CPETR_2$) are localized within the Williams–Beuren Syndrome deletion. *American Journal of Human Genetics, 54,* 453–459.

Peoples, R., Perez-Jurado, L., Wang, Y. K., Kaplan, P., & Francke, U. (1996). The gene for replication factor C subunit 2 (RFC2) is within the 7q11.23 Williams syndrome deletion. *American Journal of Human Genetics, 58,* 1370–1373.

Perez-Jurado, L. A., Wang, Y. K., Peoples, R., Coloma, A., Cruces, J., & Francke, U. (1998). A duplicated gene in the breakpoint regions of the 7q11.23 Williams–Beuren syndrome deletion encodes the initiator binding protein TFII-I and BAP-135, a phosphorylation target of BTK. *Human Molecular Genetics, 7,* 325–334.

Reilly, J. S., Klima, E. S., & Bellugi, U. (1990). Once more with feeling: Affect and language in atypical populations. *Development and Psychopathology, 2,* 367–391.

Reiss, A. L., Eliez, S., Schmitt, E. J., Strauss, E., Lai, Z., Jones, W. L., & Bellugi, U. (this volume). Neuroanatomy of Williams syndrome: A high-resolution MRI study.

Robinson, W. P., Waslynka, J., Bernasconi, F., Wang, M., Clark, S., Kotzot, D., & Schinzel, A. (1996). Delineation of 7q11.2 deletions associated with Williams–Beuren syndrome and mapping of a repetitive sequence to within and to either side of the common deletion. *Genomics, 34,* 17–23.

Tassabehji, M., Metcalfe, K., Donnai, D., Hurst, J., Reardon, W., Burch, M., & Read, A. P. (1997). Elastin: Genomic structure and point mutations in patients with supravalvular aortic stenosis. *Human Molecular Genetics, 7,* 1029–1036.

Tassabehji, M., Metcalfe, K., Karmiloff-Smith, A., Carette, M. J., Grant, J., Dennis, N., Reardon, W., Splitt, M., Read, A., & Donnai, D. (1999). Williams syndrome: Use of chromosomal microdeletions as a tool to dissect cognitive and physical phenotypes. *American Journal of Human Genetics, 64,* 118–125.

Wang, Y. K., Samos, C. H., Peoples, R., Perez-Jurado, L. A., Nusse, R., & Francke, U. (1997). A novel human homologue of the *Drosophila* frizzled wnt receptor gene binds wingless protein and is in the Williams syndrome deletion at 7q11.23. New Gene called F1/27/1993. *Human Molecular Genetics, 6,* 465–472.